A Comparative Investigation on Adsorption Performances of Activated Carbon Prepared from Coconut Husk Fiber and Commercial Activated Carbon for Acid Red 27 Dye

Hatem A. Al-Aoh[*], M. Jamil Maah, Rosiyah Yahya and M. Radzi Bin Abas

Department of Chemistry, Faculty of Science, University of Malaya, 50603 Kuala Lumpur, Malaysia

*Corresponding author: Tel: +60 176243656; E-mail: issa_hatem2@yahoo.com

The adsorption of acid red 27 dye on activated carbon fiber and granular activated carbon were studied in a batch system. The effects of initial concentration, agitation time, solution pH and temperature were examined. Adsorption isotherms were described using both the Langmuir and Freundlich models at three different temperatures. It was found that, the Langmuir model fits well with the experimental data at each temperature. The pseudo-first-order, pseudo-second-order and intra-particle diffusion models were used to examine the kinetics data. The results obtained showed that the empirical kinetics data of activated carbon fiber at 60 and 100 mg/L were well described only by the pseudo-second-order model. The intraparticle diffusion was involved at 200 mg/L for activated carbon fiber and at each tested concentration for granular activated carbon. It was observed that activated carbon fiber has a higher adsorption capacity and adsorption rate than that of granular activated carbon. Adsorption thermodynamic parameters were estimated and the values of ΔH°, ΔS° and ΔG° obtained indicate that the adsorption of acid red 27 on activated carbon fiber and granular activated carbon were exothermic and spontaneous processes.

Key Words: Adsorption, Isotherm, Kinetic, Thermodynamic, Coconut husk, Activated carbon, Acid red 27 dye.

INTRODUCTION

Azo dyes represent the largest and the most important class of the commercial dyes which are generally used in textile and other industries[1]. Acid red 27 dye (AR 27) is the most common category among all of these dyes[2]. It is usually used as colourant in textile for wool and silk, colour photography, paper industries and in food[2-4]. It was discovered that 12 % of the dye is released during the dyeing processes into wastewater[5]. It was also found by studies conducted in Russia that acid red 27 is a carcinogen[6]. The interaction of acid red 27 dye with human hemoglobin in solution was investigated by Wang *et al.*[6]. They concluded that the binding of acid red 27 with these proteins has toxicological importance. The disposal of the coloured wastewaters poses a major problem for the industry as well as a threat to environment[7]. Therefore, various methods, *e.g.*, ozonation[8], photocatalytic degradation[1,2,9-12], oxidation[13] and others were applied to remove acid red 27 from wastewaters before their discharge to the environment. Although the adsorption technique was used for the removal of acid dyes such as, acid red 73[14], acid red 18[15,16], acid red 14[17,18], acid red 88[19], acid red 97[20], ARB[21] and ARG[22]. There seems to be only two attempts in the literature that have been carried out by Phan *et al.*[23] and Metivier-Pignon *et al.*[24] on the adsorption of acid red 27 dye. Phan and his co-worker studied adsorption of acid red 27 onto activated carbon prepared from low cost materials, jute and coconut husk fibers. They found that the maximum adsorption capacities of 62.18 and 49.60 mg/g for activated carbon prepared from jute and coconut fibers, respectively. Metivier-Pignon *et al.*[24] found higher adsorption capacity for the adsorption of acid red 27 by activated carbon fiber produced from cloths, which are more expensive than the raw materials used for the production of the commercial activated carbon. Therefore, additional work is required to improve the potential of the inexpensive activated carbon prepared from coconut husk fiber towards acid red 27 dye. Thus, the main aim of this work was to investigate adsorption of acid red 27 dye on activated carbon fiber (ACF) prepared from coconut husk under optimal conditions. The second objective was to compare the adsorption performance of activated carbon fiber and commercial granular activated carbon (GAC). The effect of adsorption parameters, adsorption isotherms, kinetic and thermodynamics were investigated in a batch system.
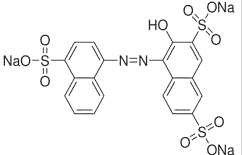
EXPERIMENTAL

Preparation of activated carbon fiber: The fibers of coconut husk were used for the preparation of activated carbon fibers under optimal conditions using a horizontal tube furnace.

The optimized experimental conditions were determined prior to the use of 800 ºC as activation temperature, 50 % w/v ZnCl₂ concentration, 200 cm³/min nitrogen flow rate, 2 h activation time and 300 ºC carbonization temperature. The produced sample was washed once with 1.5 M solution HCl and several times with deionized water until the pH of the washing effluent reached 6-7. Finally, the sample was dried at 110 ºC over night in an oven and stored in a dessicator for other uses. The activated carbon fiber produced in this work and the commercial activated carbon (in the granular form) are described as activated carbon fiber and commercial granular activated carbon, respectively.

Characterization of the adsorbents: The specific surface areas of the activated carbon fiber and commercial granular activated carbon were determined by N_2 adsorption (at 77.40 K), using a surface analyzer (Sorptomatic Thermo Finnigan 1990, USA). The *t*-method was used to measure the pore structure of these adsorbents. The pH at the point of zero charge (pHZPC) was determined by a batch equilibrium method. The Fourier Transform Infrared spectroscopy (FT-IR) (Perkin Elmer-2000 FT-IR) measurements were performed to quantify the surface functional groups of these two activated carbons. The surface morphology of the activated carbon fiber and commercial granular activated carbon were examined by scanning electron microscopy (LEO 1455 VP, England).

Preparation of dye solutions: The dye of acid red 27 (AR 27) with chemical and physical properties represented in Table-1 was supplied by Sigma-Aldrich, USA, APEO. The stock solution (10000 mg/L) of acid red 27 was prepared in deionized water. The desired concentrations of the adsorption solutions were obtained by dilution.

TABLE-1
STRUCTURE AND CHARACTERISTICS OF ACID RED 27 DYE

Structure	Other names	CI number	λ_{max} (nm)	M_w (g/mol)
	Amaranth Azorubin S	16185	420	604.47

Adsorption experiments

Impact of the initial concentration of the adsorbate: To investigate the effect of the initial concentration, adsorption of acid red 27 on activated carbon fiber and commercial granular activated carbon was carried out at various concentrations of the dye solutions (20, 40, 60, 80, 100, 200, 300, 400, 500, 600, 700, 800, 900 and 1000 mg/L) using a fixed amount of adsorbent (0.03 g) at initial pH, agitation speed 150 rpm and 30 ± 1 ºC for 4 days to achieve equilibrium. The samples were filtered and the final concentrations of acid red 27 in the filtrate were measured by the UV-visible spectrophotometer (Shimadzu, Japan) at the maximum wave length 420 nm. The equilibrium adsorption amounts were computed from eqn. 1.

$$q_e = \frac{(C_o - C_e)V}{W} \qquad (1)$$

where C_o and C_e (mg/L) are the initial and final concentrations of acid red 27, respectively, W (g) is the mass of adsorbent

used, q_e (mg/g) is the adsorption amount at equilibrium and V (L) is the volume of the solution.

Isotherm studies: Adsorption of 200, 300, 400, 500 and 600 mg/L of acid red 27 solution onto fixed amounts (0.03 g) of activated carbon fiber and granular activated carbon were carried out at 30, 45 and 60 ºC in a batch system. These experiments were performed by adding 25 mL of each solution to 30 mL amber bottles each of which contained the required amount of activated carbon fiber or granular activated carbon. The amber bottles were sealed and placed in an incubator shaker. The bottles were shaken at the initial pH and at an agitation speed 150 rpm for 4 days to reach equilibrium. The mixtures were filtered and the final concentrations of acid red 27 in the filtrate were measured by UV-visible spectrophotometer (Shimadzu, Japan) at the acid red 27 dye maximum wave length (420nm). Eqn. 1 was used for calculation of the amounts of this dye adsorbed at equilibrium. The results obtained were used for determination of the adsorption capacities and thermodynamic parameters. The effect of temperature was also investigated using these results.

Kinetic studies: To investigate the effect of the contact time and adsorption kinetics, adsorption of 60, 100 and 200 mg/L of acid red 27 onto the prepared activated carbon fiber and the commercial granular activated carbon were performed at the original pH, at an agitation speed of 150 rpm at 30 ± 1 ºC for various time periods. The other experimental processes were carried out as mentioned earlier with the isotherm studies. The adsorption amount at any time t (min) was computed by the following equation:

$$q_t = \frac{(C_0 - C_t)V}{W} \qquad (2)$$

where, q_t (mg/L) is the amount of acid red 27 adsorbed at time t (mg/g). C_o and C_t (mg/L) are the liquid phase concentration at initial and any time t, respectively. V is the volume of the solution (L) and W (g) is the mass of adsorbent.

Effect of solution pH: The solutions of acid red 27 dye with initial concentration of 400 mg/L and various initial pH values (1-11) were prepared. The pH of each solution was adjusted to the required value by adding HCl or NaOH solutions before mixing the adsorbent using a pH meter (Model: Ross FE 20, USA). 25 mL of each solution was added to the 30 mL amber bottles containing 0.03 g of the prepared activated carbon fiber. The bottles were sealed and put in a rotational shaker and shaken at room temperature (30 ± 1 ºC) and at an agitation speed of 150 rpm for 4 days. The solid adsorbents were separated from the mixtures by filtration using filter papers. The final concentration of the acid red 27 and the equilibrium adsorption amount were determined according to the isotherm studies.

For comparison, all the procedures mentioned above were repeated with the commercial granular activated carbon.

RESULTS AND DISCUSSION

Characterization of the activated carbons: The results of the surface analyzer and pHZPC of the activated carbon fiber and granular activated carbon are summarized in Table-2. It can be observed from this Table that activated carbon fiber has a higher surface area, total pore volume, mesopore volume

TABLE-2
CHARACTERISTICS OF THE ACF AND ACG

Type of activated carbon	Activated carbon fiber	Commercial granular activated carbon
Specific surface area (m²/g)	5435	1061
Total pore volume (cm³/g)	4.043	0.559
Micropore volume (cm³/g)	1.479	0.328
Mesopore volume (cm³/g)	2.564	0.231
Average pore diameter (Å)	29.76	21.06
Micropore (%)	36.582	58.68
Mesopore (%)	63.418	41.32
pH$_{ZPC}$	7.6	6.7

and percentage mesopore higher than that of granular activated carbon. This indicates that the prepared activated carbon fiber has higher adsorptive properties than that of the commercial granular activated carbon.

Figs. 1 and 2 represent the SEM photograph of activated carbon fiber produced by this study and commercial granular activated carbon. It can be seen from these figures that the majority of pores on the surface of these adsorbents are mesopores which are more effective in dye adsorption. Moreover, these figures demonstrate that the number of pores on the surface of activated carbon fiber higher than that of granular activated carbon. The results observed in this part are in agreement with the results from the surface analyzer.
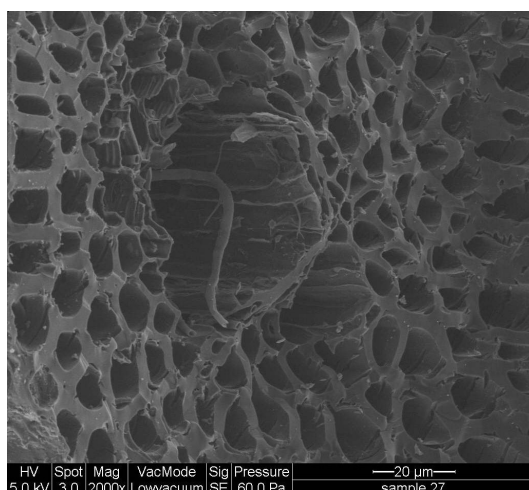

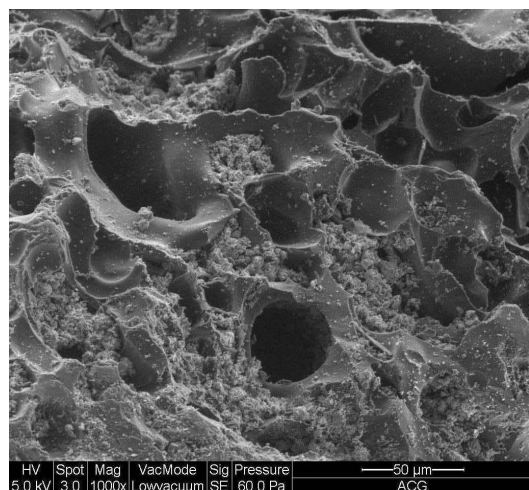Fig. 1. SEM image of the prepared activated carbon fiber

Fig. 2. SEM image of the commercially available granular activated carbon

The FT-IR experiments were performed to evaluate qualitatively the functional groups on the surface of activated carbon fiber and granular activated carbon. The spectra obtained are shown in Fig. 3. It is shown in Fig. 3, that the broad band at 3343.25 cm⁻¹ can be attributed to the presence of a hydroxyl group. The band located at around 2949.53 cm⁻¹ corresponds to C-H vibration stretching. The absorption peak recorded in the region of 1057.34 cm⁻¹ is attributed to the symmetrical angular deformation of ethers[25]. There are two absorption peaks that can be observed at around 3434.43 and 1633.36 cm⁻¹ in commercial granular activated carbon. These two peaks are attributed to a hydroxyl group and axial deformation of carbonyl groups (C=O), respectively.
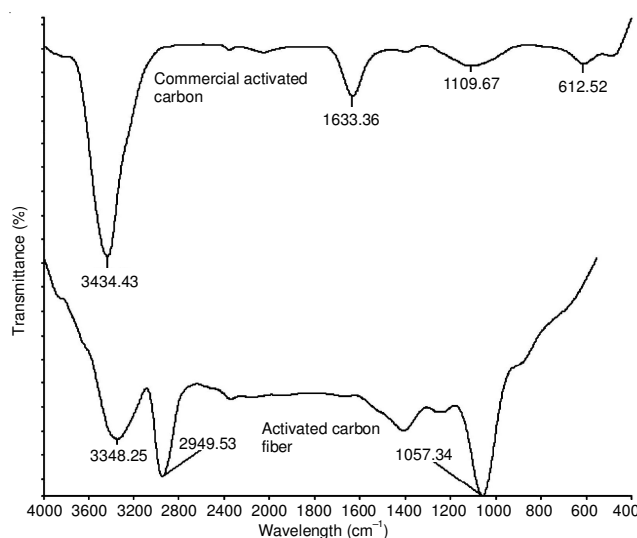

Fig. 3. FT-IR graph of the prepared activated carbon fiber and the commercial granular activated carbon

Adsorption studies

Effect of initial dye concentration on acid red 27 adsorption: In this work, the effects of the initial dye concentration on the adsorption capacity of acid red 27 were investigated in the range of 20-1000 mg/L for both activated carbon fiber and granular activated carbon. The results obtained are represented in Fig. 4. As shown in this figure, the amount of acid red 27 dye adsorbed onto activated carbon fiber or granular activated carbon increases as the initial dye concentration is increased. This is due to increasing the driving force which can overcome all the mass transfer resistances of the adsorbate molecules between the liquid and solid phases[17,26]. It can also be observed from Fig. 4 that the adsorption amount of this dye is constant over 600 and 700 mg/L for granular activated carbon and activated carbon fiber, respectively. This may come from the saturation of the adsorption sites on the surfaces of these carbons as the concentration of acid red 27 is increased over 600 and 700 mg/L[17,26]. Moreover, it can be seen from Fig. 4 that the adsorption capacity of this dye on the prepared activated carbon fiber is double that of the granular activated carbon. This can be explained by the specific surface area, pore diameter, total pore volume and higher mesopore volume and percentage of activated carbon fiber compared with granular activated carbon (Table-2). Similar results were observed in the literature for the adsorption of azo dye and acid blue 113
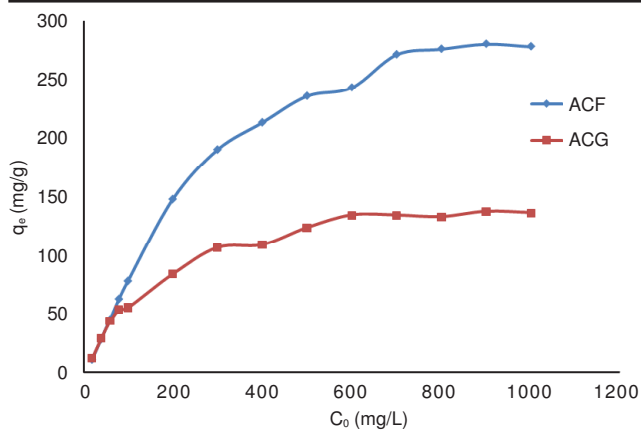
Fig. 4.   Effect of initial concentration on the adsorption capacity of acid red 27 dye onto activated carbon fiber and granular activated carbon

onto activated carbon prepared from waste rubber tires and from commercial activated carbon[26].

Isotherm data analysis: Isotherm data for the adsorption of acid red 27 onto activated carbon fiber and granular activated carbon were applied to the Langmuir and Freundlich models. The results of the linear form of these two models were used to determine the fit of the models. The linearized forms of the Langmuir and Freundlich models are represented in eqns. 3 and 4, respectively.

$$\frac{C_e}{q_e} = \frac{1}{q_{max}K_L} + \frac{C_e}{q_{max}} \tag{3}$$

$$\ln q_e = \ln K_F + \frac{1}{n}\ln C_e \tag{4}$$

where, q_e is the amount of an adsorbate adsorbed at equilibrium (mg/g), q_{max} the maximum adsorption capacity corresponding to a complete monolayer coverage on the surface (mg/g), C_e is the concentration of the adsorbate at equilibrium (mg/L). K_L is the Langmuir constant related to the energy or net enthalpy of adsorption. K_F is the Freundlich constant related to the adsorption capacity. $1/n$ is another constant in the Freundlich model related to the favorability of adsorption. Since, if the value of $1/n$ is between 0 and 1, this indicates that the adsorption is favorable[27].

The essential characteristics of the Langmuir isotherm can be expressed by a dimensionless factor called the equilibrium parameter R_L defined by eqn. 5[28].

$$R_L = \frac{1}{1 + K_L C_0} \tag{5}$$

where, K_L is the Langmuir constant and is the highest adsorbate concentration. The value of R_L indicates the type of isotherm,

either unfavorable ($R_L > 1$), linear ($R_L = 1$), favorable ($0 < R_L < 1$) or irreversible ($R_L = 0$).

The obtained values of the isotherm parameters, correlation coefficient (R^2) and R_L values are listed in Table-3.

Figs. 5 and 6 demonstrate that the plots of Langmuir model for activated carbon fiber and granular activated carbon at three different temperatures are linear over the whole concentration range which were used. It can also be seen from Table-3 that the correlation coefficients of the Langmuir model varied from 0.986-0.997 for activated carbon fiber and from 0.912-0.984 for granular activated carbon.
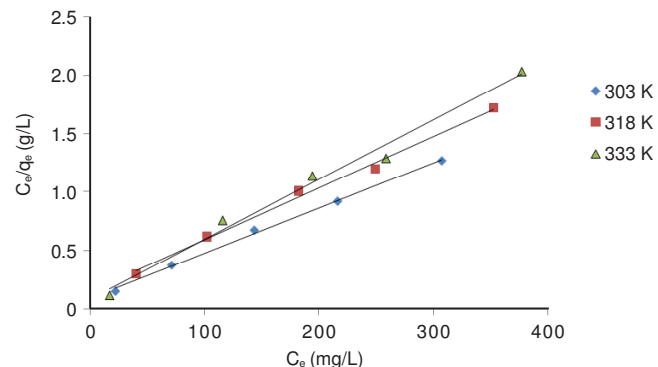

Fig. 5.   Langmuir isotherm model at three different temperatures for adsorption of acid red 27 dye on activated carbon fiber
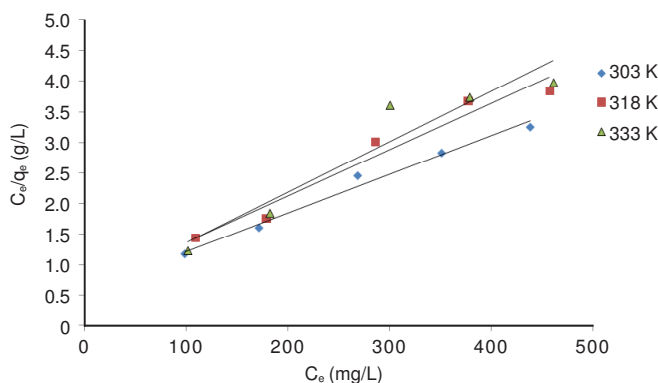

Fig. 6.   Langmuir isotherm model at three different temperatures for adsorption of acid red 27 dye on commercial granular activated carbon

In contrast, the plots of the Freundlich model (Figs. 7 and 8) at three different temperatures for both adsorbents are not linear. Moreover, the correlation coefficients of Freundlich model ranged from 0.581 to 0.993 for activated carbon fiber and from 0.476 to 0.949 for granular activated carbon.

These results suggest that the Langmuir model satisfactorily fits the adsorption of acid red 27 on the prepared activated

TABLE-3
LANGMUIR, FREUNDLICH PARAMETERS AND SEPARATION FACTORS (RL) FOR THE ADSORPTION OF ACID RED 27 ONTO
ACTIVATED CARBON FIBER (ACF) AND GRANULAR ACTIVATED CARBON (ACG) AT THREE DIFFERENT TEMPERATURES

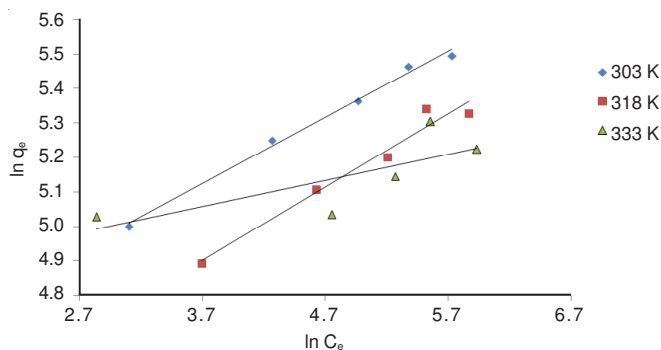| Adsorbent	Temperature (°C)	Langmuir isotherm				Freundlich isotherm			
		q_{max} (mg/g)	K_L (L/mg)	R_L	R^2	K_F (mg/g)(L/mg)$^{1/n}$	$1/n$	n	R^2
ACF	30	333.33	0.034	0.047	0.997	82.27	0.192	5.21	0.993
	45	250	0.023	0.058	0.994	60.95	0.213	4.69	0.966
	60	200	0.064	0.026	0.986	118.75	0.075	13.33	0.581
ACG	30	166.67	0.010	0.143	0.984	22.49	0.291	3.44	0.949
	45	142.86	0.011	0.132	0.959	24.58	0.249	4.02	0.764
	60	125	0.015	0.100	0.912	38.86	0.162	6.17	0.476

Fig. 7. Freundlich isotherm model at three different temperatures for adsorption of acid red 27 on activated carbon fiber
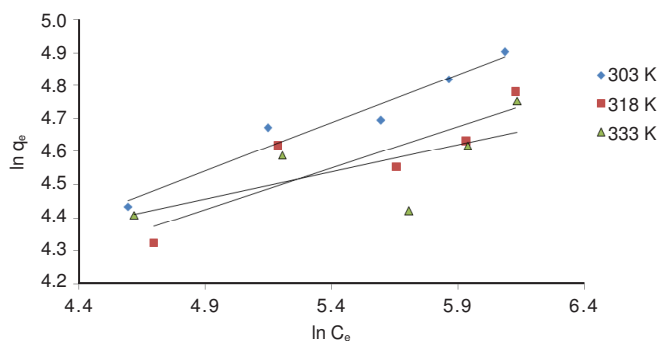

Fig. 8. Freundlich isotherm model at three different temperatures for adsorption of acid red 27 on granular activated carbon
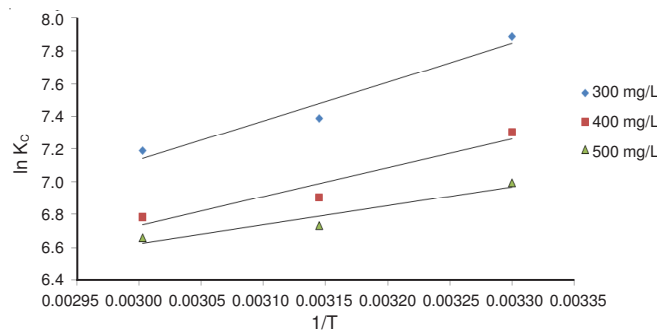

Fig. 9. Variation of ln K_C with 1/T for the adsorption of acid red 27 on activated carbon fiber at three different initial concentrations
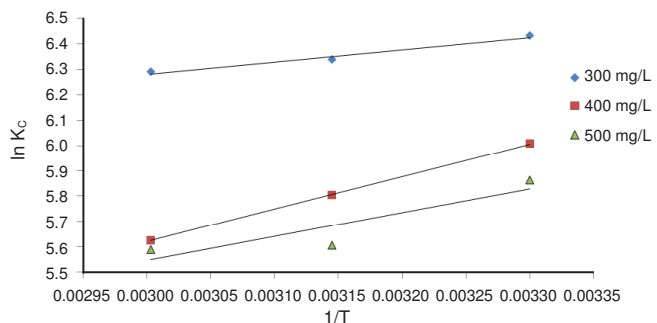

Fig. 10. Variation of ln K_C with 1/T for the adsorption of acid red 27 on granular activated carbon at three different initial concentrations

carbon fiber and the commercial granular activated carbon. Similar results were observed in the adsorption of acid blue 113 on the activated carbon prepared from waste rubber tires and commercially activated carbon[26].

The values of R_L (Table-3) in the case of activated carbon fiber are smaller than that of commercial granular activated carbon at each temperature, indicating that the adsorption of this dye on activated carbon fiber is more favorable than that of granular activated carbon. Furthermore, it can be observed from Table-3 that the prepared activated carbon fiber at each temperature adsorption capacity is higher than the adsorption capacity of the commercial granular activated carbon. This is due to the superior surface area and porosity of the prepared activated carbon fiber.

Effect of temperature: Adsorption isotherms of acid red 27 dye on activated carbon fiber and granular activated carbon were investigated at 30, 45 and 60 ºC. The results of this investigation are summarized in Table-3. It can be seen from this Table that the adsorption capacities of activated carbon fiber and granular activated carbon decrease with increasing the adsorption temperature. This indicates that the adsorption of acid red 27 onto activated carbon fiber and granular activated carbon is an exothermic process[29,30]. It was reported by Ozcan and Ozcan[31] that the amount of adsorption of the acid red 57 on a surfactant-modified sepiolite decreased with increasing temperature.

Determination of thermodynamic parameters: The enthalpy ($\Delta H°$) and entropy ($\Delta S°$) change values were computed from slopes and intercepts of the lines plotted (Figs. 9 and 10) according to eqn. 6 while the values of the free energy change ($\Delta G°$) were calculated at three different temperature from eqn. 7.

$$\ln K_C = -\frac{\Delta H°}{RT} + \frac{\Delta S°}{R} \qquad (6)$$

$$K_C = \frac{q_e}{C_e} \times P$$

$$\Delta G° = \Delta H° - T\Delta S° \qquad (7)$$

where, R is the universal gas constant (8.314 J/K mol)), T is the adsorption temperature (K) and P is the density of the solution (P = 1000 g/L). The calculated values of these parameters are summarized in Table-4. The negative values of $\Delta H°$ indicate that the adsorption of acid red 27 onto activated carbon fiber and granular activated carbon is an exothermic in nature[30]. The heat of adsorption ($\Delta H°$) for activated carbon fiber at each concentration is higher than that of granular activated carbon, indicating that the adsorption of acid red 27 onto activated carbon fiber is more temperature-sensitive[30]. The positive values of entropy change ($\Delta S°$) indicates that the raised randomness during the adsorption of acid red 27 onto activated carbon fiber and granular activated carbon. is due to liberation of water molecules from the hydrated species of the adsorbent[32]. The negative values of the free energy change ($\Delta G°$) suggest that the adsorption of this dye on these two adsorbents is a spontaneous process. This means no energy from outside the adsorption system is required[32]. The results obtained in this work are in agreement with the results observed in the adsorption of acid oranges 7 and 10 onto ethylene-diamine-modified magnetic chitosan nanoparticles[32].

Effect of pH: The interactions between the functional groups of the adsorbent surface and the adsorbate are affected by the solution pH[15]. Therefore, this parameter is very important in the adsorption process. In this work, the effects of pH on the adsorption of acid red 27 onto activated carbon fiber and

TABLE-4
THERMODYNAMIC PARAMETERS FOR THE ADSORPTION OF ACID RED 27 ONTO
ACTIVATED CARBON FIBER (ACF) AND GRANULAR ACTIVATED CARBON (ACG)

Adsorbent	Concentration (mg/L)	ΔH^o (kJ/mol)	ΔS^o (KJ/mol)	ΔG^o (KJ/mol)			
				303 K	318 K	333 K	R^2
ACF	300	-19.73	0.0001	-19.7603	-19.7618	-19.7633	0.953
	400	-14.72	0.0118	-18.2954	-18.4724	-18.6494	0.925
	500	-9.52	0.0265	-17.5495	-17.947	-18.3445	0.919
ACG	300	-3.95	0.0404	-16.1912	-16.7972	-17.4032	0.974
	400	-10.73	0.0145	-15.1235	-15.341	-15.5585	0.999
	500	-7.83	0.0226	-14.6778	-15.0168	-15.3558	0.815

granular activated carbon have been demonstrated in Fig. 11. As shown in this figure, the maximum adsorption capacity was at pH = 1 for both activated carbon fiber and granular activated carbon. It can also be seen from Fig. 11 that the adsorption amount decreases with increasing pH. Where, pHZPC is the pH value at which the surface charge of the adsorbent equals to zero[15]. The pHZPC was investigated in this work and found to be 7.8 and 6.4 for activated carbon fiber and granular activated carbon, respectively. The adsorbent surface in the solution is positively charged at solution pH < pHZPC and negatively charged if the solution pH is higher than pHZPC[33]. it was reported previously that some acidic dyes such as acid yellow and acid red 18 are negatively charged even in highly acid solution due to the presence of sulfonic groups and N=N bonds in their structure[34]. Thus, increasing pH from 1 until the value equal to pHZPC reduces the electrostatic attraction between the positive charge of the adsorbent surface and the negative ions of acid red 27 whereas, increasing the solution pH over pHZPC increases the electrostatic repulsion between the negative ions of this dye and the negative surface of the adsorbent. In both the cases mentioned above, the adsorption amount would be decreased. Similar trends were reported in the literature for adsorption of food dyes such as acid yellow 6, acid yellow 23 and acid red 18 on activated carbon prepared from flamboyant pods[15].
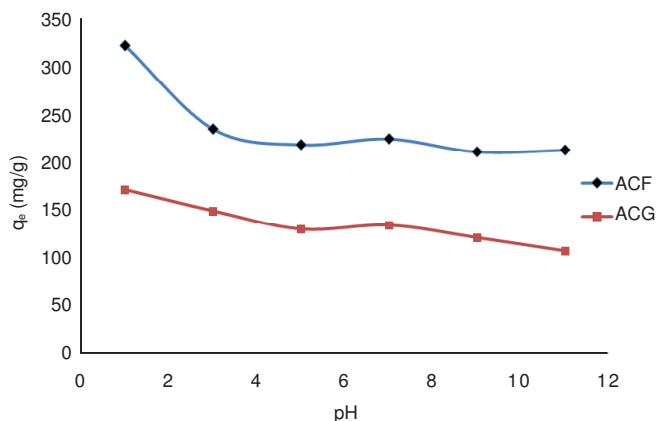
Fig. 11. Effect of pH on the adsorption of acid red 27 onto activated carbon fiber and granular activated carbon

Effect of contact time: The plots of q_t (mg/g) against t (min) for the adsorption of acid red 27 at different initial concentrations by activated carbon fiber and granular activated carbon are presented in the Figs. 12 and 13, respectively. Fig. 12 demonstrates that the amount of acid red 27 uptake by activated carbon fiber increased with increased agitation time and reached
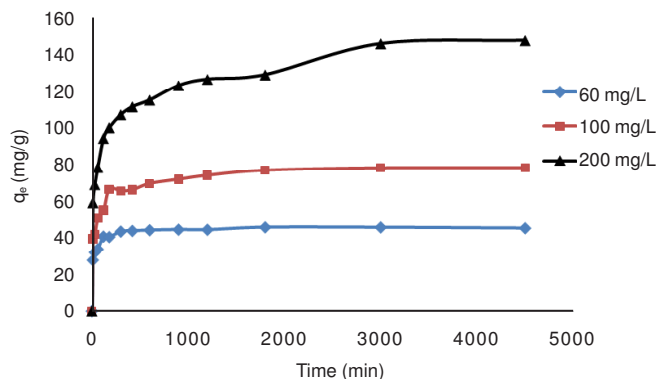
Fig. 12. Effect of the adsorption time on the uptake of acid red 27 by activated carbon fiber at three initial concentrations (60, 100 and 200 mg/L)
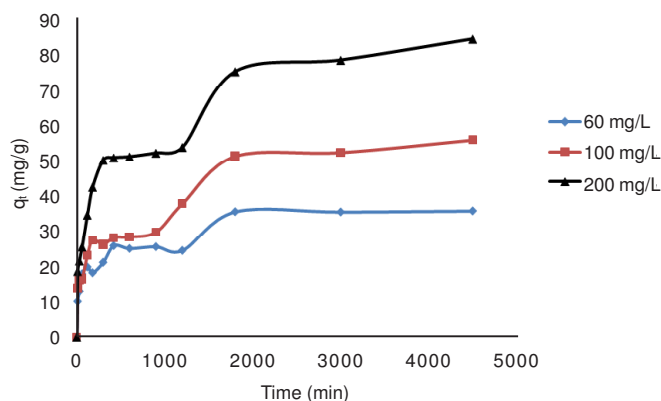
Fig. 13. Effect of the adsorption time on the uptake of acid red 27 by granular activated carbon at three initial concentrations (60, 100 and 200 mg/L)

equilibrium at 180 min for the solutions of 60 and 100 mg/L. it can also be seen from Fig. 12 that the adsorption of 200 mg/L acid red 27 solution by the same adsorbent sharply increased when the time is increased from 10 to 180 min, slightly increased in the range of 180 to 1800 min and the maximum adsorption was achieved at 4500 min. While, the amount of acid red 27 adsorbed onto the commercial granular activated carbon rapidly increased when the adsorption contact time increased from 10 to 420 min, it remained constant until 1200 min and the maximum adsorption was obtained in 1800 min (Fig. 13). This indicates that the acid red 27 molecules at first were adsorbed rapidly by the mesopores until this type of pores were saturated. It takes a longer time for these molecules to be adsorbed by the micropores. The results obtained confirm that the adsorption rate of the prepared activated carbon fiber is higher than of granular activated carbon. This is due to the higher average pore diameters of activated carbon fiber (Table-2).

TABLE-5
PSEUDO-FIRST AND PSEUDO-SECOND ORDER PARAMETERS AND EXPERIMENTAL QE VALUES FOR THE
ADSORPTION OF ACID RED 27 DYE BY ACF AND ACG AT DIFFERENT INITIAL CONCENTRATIONS AND 30 ± 1 ℃

Adsorbent	C_0 (mg/L)	$q_{e,exp}$ (mg/g)	Pseudo-first-order kinetic model			Pseudo-second-order kinetic model			
			$q_{e,cal}$ (mg/g)	K_1 (h^{-1})	R^2	$q_{e,cal}$ (mg/g)	K_2 (g/mg min)	R^2	Rate
ACF	60	45.51	11.19	0.0023	0.882	47.62	0.00120	0.999	0.057
	100	78.33	28.84	0.0023	0.770	76.92	0.00047	0,998	0.036
	200	148.12	70.15	0.0000	0.872	125	0.00025	0.999	0.031
ACG	60	35.69	20.46	0.0000	0.824	27.03	0.00071	0.984	0.019
	100	55.72	36.90	0.0000	0.661	30.30	0.00094	0.997	0.028
	200	84.26	57.68	0.0000	0.799	58.82	0.00026	0.995	0.015

Kinetic data analysis: The data found from the experiments of the effect of contact time studies were further used to investigate the adsorption kinetics. Three kinetic models, namely, pseudo-first-order, pseudo-second-order[35] and intraparticle diffusion models were applied to determine the adsorption rate constant and equilibrium adsorption capacity at three different initial concentrations. The linear form of the pseudo-first-order model is:

$$\log(q_e - q_t) = \log q_e - K_1 \frac{t}{2.303} \qquad (8)$$

where, q_e and q_t (mg/g) are the adsorption amount at the point of equilibrium and any time t (min), respectively. K_1 (min^{-1}) is the rate constant of the adsorption which can be computed from the slope of the straight-line plot of eqn. 8. The values of q_e can be obtained from the intercepts of these straight-line plots.

The linear expression of the pseudo-second-order model is:

$$\frac{t}{q_t} = \frac{1}{K_2 q_e^2} + \frac{t}{q_e} \qquad (9)$$

where, K_2 (g/mg min) is the rate constant of this model which can be determined from the intercept of the straight-line plot of t/q_t *verses* t, whereas, q_e was calculated from the slope of this plot.

The intraparticle diffusion equation is:

$$q_t = K_{dif} \sqrt{t} + C \qquad (10)$$

where, K_{dif} (mg/g min)$^{1/2}$ is the rate constant of the intraparticle diffusion which can be calculated from the slope of the straight-line plot of q_t against $t^{1/2}$ and the intercept of this plot is equal to the parameter C which gives information about the thickness of the boundary-layer[36]. The plots of these kinetic models for the adsorption of acid red 27 by activated carbon fiber and granular activated carbon are represented in the Figs. 14-19. The calculated kinetic parameters in this work are summarized in Tables 5 and 6. According to the correlation coefficient (R^2) values of the pseudo-first-order kinetic model (Table-5) and the calculated q_e values, which are too low compared to experimental q_e values, it can be suggested that the adsorption of acid red 27 by activated carbon fiber and granular activated carbon cannot be described by this kinetic model. The R^2 values and the agreement between the experimental q_e values and the calculated ones (Table-5) for the adsorption at 60 and 100 mg/L of this dye suggest that the adsorptions of these two concentrations onto activated carbon fiber follow the pseudo-second-order kinetic model. Although, the correlation coeffi-
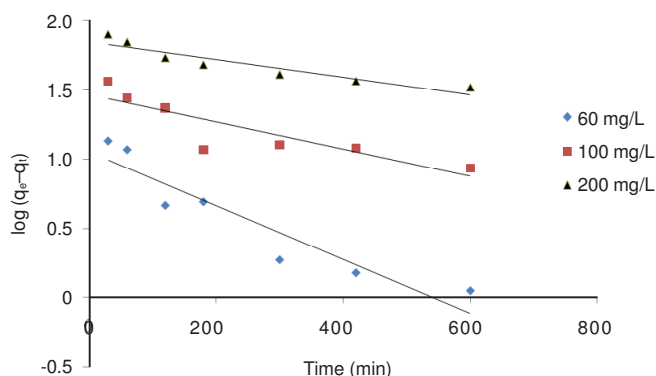

Fig. 14. Pseudo first-order kinetics plots for the adsorption of acid red 27 onto activated carbon fiber at different initial concentrations
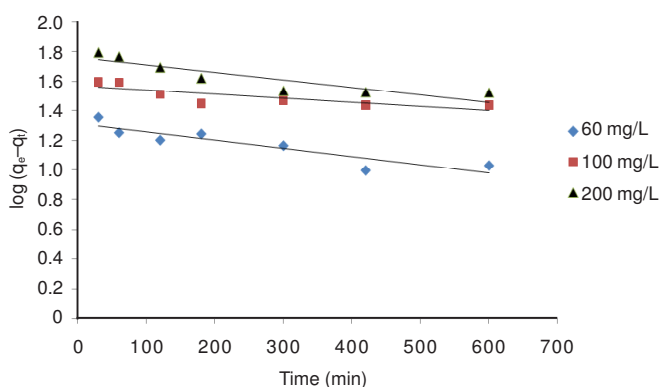

Fig. 15. Pseudo first-order kinetics plots for the adsorption of acid red 27 onto granular activated carbon at different initial concentrations
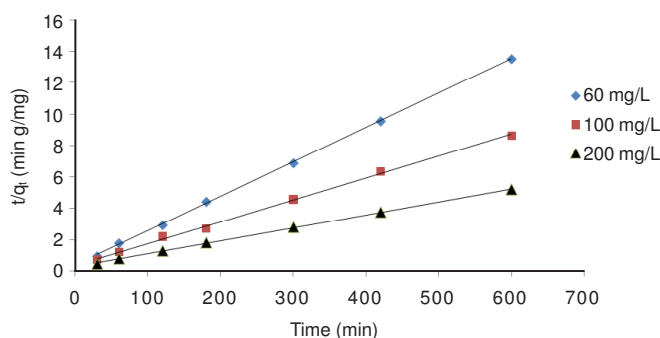

Fig. 16. Pseudo second-order kinetics plots for the adsorption of acid red 27 onto activated carbon fiber at different initial concentrations

cient for the adsorption of 200 mg/L is 0.999, the calculated equilibrium adsorption capacity value (125 mg/g) is not in agreement with that obtained experimentally (148.12 mg/g). Therefore, these results demonstrate that the pseudo-second-order kinetic model cannot describe well the adsorption process
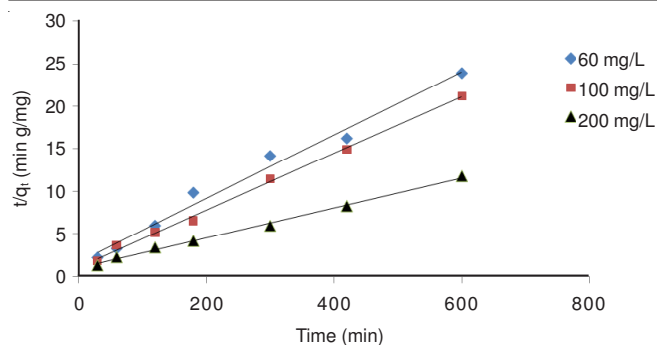
Fig. 17. Pseudo second-order kinetics plots for the adsorption of acid red 27 onto granular activated carbon at different initial concentrations
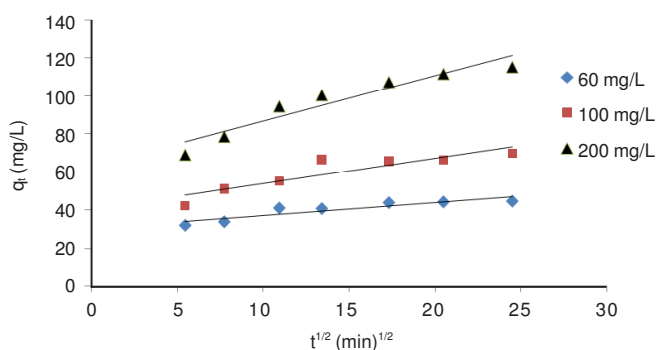

Fig. 18. Intra-particle diffusion for the adsorption of acid red 27 onto activated carbon fiber at different initial concentrations
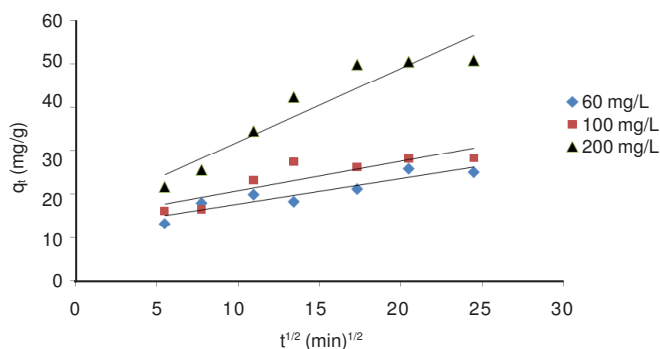

Fig. 19. Intra-particle diffusion for the adsorption of acid red 27 onto granular activated carbon at different initial concentrations

of acid red 27 at higher concentration (200 mg/L). Moreover, R^2 values of the intraparticle diffusion (Table-6) are 0.820, 0.813 and 0.911 for the adsorption of 60, 100 and 200 mg/L of acid red 27 onto activated carbon fiber, respectively. This confirms that the intraparticle diffusion was only involved in the adsorption process at 200 mg/L. This means that at higher concentrations of acid red 27, some molecules are adsorbed rapidly by the mesopores available on the surface of activated carbon fiber until this type of pores become saturated and a longer time is required for adsorption of the other molecules by micropores. Despite, the higher values of R^2 for the pseudo-second-order in the case of acid red 27 adsorption on granular activated carbon, there is no agreement between the calculated q_e values and the experimental q_e values (Table-5). These results assume that the adsorption process of AD 27 by granular activated carbon does not fit well with the pseudo-second-order kinetic model. The R^2 values of the intraparticle diffusion

(Table-6) are higher than that of the pseudo-first-order kinetic model. Figs. 13 and 19 indicate that the intraparticle diffusion mechanism is involved in the adsorption of this dye onto granular activated carbon at each concentration which had been used in this work. This can be explained by the small value of the percentage of available mesopores (Table-2) on the surface of granular activated carbon compared to that of the activated carbon fiber. Therefore, intraparticle diffusion was involved in the adsorption of this dye on activated carbon fiber at 200 mg/L and at each concentration in the case of granular activated carbon.

TABLE-6
PARAMETER VALUES OF INTRA-PARTICLE DIFFUSION
MODEL FOR THE ADSORPTION OF ACID RED 27 DYE
BY ACF AND ACG AT DIFFERENT INITIAL
CONCENTRATIONS AND 30 ± 1 ºC

Sample	$C_{0 (mg/L)}$	$q_{e,exp}$ (mg/g)	Intra-particle diffusion		
			K_{dif} $(mg/h^{1/2}g)$	C	R^2
ACF	60	45.51	0.659	30.51	0.820
	100	78.33	1.345	40.23	0.813
	200	148.12	2.404	60.41	0.911
ACG	60	35.69	0.591	11.71	0.854
	100	55.72	0.685	13.90	0.778
	200	84.26	1.699	15.15	0.891

It can be observed from Table-5 that the rate of acid red 27 adsorption onto activated carbon fiber is higher than that of the granular activated carbon. This came from the higher average pore diameter of activated carbon fiber compared to that of the granular activated carbon as shown in Table-2.

Conclusion

Coconut husk fiber was used as a starting material for the preparation of activated carbon fiber. The physical and chemical properties of the prepared activated carbon fiber (ACF) and a commercially available granular activated carbon (ACG) were investigated. The results obtained indicated that the adsorptive properties of activated carbon fiber (for example: 5435 m^2/g surface area and 2.564 cm^3/g mesopores volume) are better than that of granular activated carbon (1061 m^2/g surface area and 0.231 cm^3/g mesopores volume). Langmuir and Freundlich models were applied to investigate the adsorption isotherms for the adsorption of acid red 27 dye at three different temperatures and it was found that the experimental data could be described well by the Langmuir model.

The maximum adsorption capacity for activated carbon fiber (333.33 mg/g) is higher than that of granular activated carbon (166.67 mg/g) at 30 ºC. The Adsorption kinetics were analyzed by pseudo-first-order, pseudo-second-order and intraparticle diffusion kinetic models. The kinetic experimental data followed the pseudo-second order model at lower concentration and the intraparticle diffusion was involved at higher concentrations in the case of activated carbon fiber. The intraparticle diffusion mechanism was involved in the adsorption of this dye onto granular activated carbon at each concentration. It was observed that the adsorption rate of acid red 27 on activated carbon fiber was higher than that for granular activated carbon. Thermodynamic parameters such as ΔHº,

ΔS° and ΔG° were calculated. The values of the parameters confirmed that the adsorption affinity of activated carbon fiber towards acid red 27 is more significant than that of granular activated carbon. In general, the results obtained suggest that the activated carbon fiber used in this work can be applied for wastewater treatment and is superior than the commercial granular activated carbon.

REFERENCES

1. N. Daneshvar, M. Rabbani, N. Modirshahla and M.A. Behnajady, *J. Photochem. Photobiol. A: Chem.*, **168**, 39 (2004).
2. P. Yadav and R.C. Meena, *Scholars Res. Library*, **2**, 66 (2010).
3. M. Karkmaz, E. Puzenat, C. Guillard and J.M. Herrmann, *Appl. Catal. B*, **51**, 183 (2004).
4. R. Zhang, C. Zhang, X. Cheng, L. Wang, Y. Wu and Z. Guan, *J. Hazard. Mater.*, **142**, 105 (2007).
5. M. Perez-Urquiza, R. Ferrer and J.L. Beltran, *J. Chromatogr. A*, **883**, 277 (2000).
6. Y.-Q. Wang, H.-M. Zhang and B.-P. Tang, *J. Photochem. Photobiol. B*, **100**, 76 (2010).
7. A.C. Silvaa, J.S. Pic, G.L. Sant'Anna Jr. and M. Dezotti, *J. Hazard. Mater*., **169**, 965 (2009).
8. A.E. Kandjani, M.F. Tabriz, N.A. Arefian, M.R. Vaezi, F. Halek and S.K. Sadrnezhaad, *Water Sci. Technol*., **6**, 1256 (2010).
9. M.A. Behnajady, N. Modirshahla, N. Daneshvar and M. Rabbani, *J. Hazard. Mater.*, **140**, 257 (2007).
10. N. Daneshvar, M. Rabbani, N. Modirshahla and M.A. Behnajady, *J. Hazard. Mater. B*, **118**, 155 (2005).
11. N. Daneshvar, M. Rabbani, N. Modirshahla and M.A. Behnajady, *Chemosphere*, **56**, 895 (2004).
12. Puttaswamy, K.N. Vinod and K.N.N. Gowda, *Dyes Pigm.*, **78**, 131 (2008).
13. M.G. Colonna, T. Caronna and B. Marcandalli, *Dyes Pigm.*, **41**, 211 (1999).
14. F. Fu, Y. Xiong, B. Xie and R. Chen, *Chemosphere*, **66**, 1 (2007).
15. A.M.M. Vargas, A.L. Cazetta, A.C. Martins, J.C.G. Moraes, E.E. Garcia, G.F. Gauze, W.F. Costa and V.C. Almeida, *Chem. Eng. J.*, **181-182**, 243 (2012).
16. T. Jesionowski, M. Pokora, W. Tylus, A. Dec and A. Krysztafkiewicz, *Dyes Pigm.*, **57**, 29 (2003).
17. Q. Baocheng, Z. Jiti, X. Xuemin, Z. Chunli, Z. Hongxia and Z. Xiaobai, *J. Environ. Sci.*, **20**, 704 (2008).
18. J.-F. Gao, J.-H. Wang, C. Yang, S.-Y. Wang and Y.-Z. Peng, *Chem. Eng. J.*, **171**, 967 (2011).
19. S.T. Akar and R. Uysal, *Chem. Eng. J.*, **162**, 591 (2010).
20. V. Gomez, M.S. Larrechi and M.P. Callao, *Chemosphere*, **69**, 1151 (2007).
21. R. Wu, J. Qu, H. He and Y. Yu, *Appl. Catal. B-Environ.*, **48**, 49 (2004).
22. D.S. Tong, C.H. Zhou, Y. Lu, H. Yu, G.F. Zhang and W.H. Yu, *Appl. Clay Sci.*, **50**, 427 (2010).
23. N.H. Phan, S. Rio, C. Faur, L.L. Coq, P.L. Cloirec and T.H. Nguyen, *J. Carbon*, **44**, 2569 (2006).
24. H. Metivier-Pignon, C. Faur and P.L. Cloirec, *Chemosphere*, **66**, 887 (2007).
25. S. Karagöz, T. Tay, S. Ucar and M. Erdem, *Bioresour. Technol.*, **99**, 6214 (2008).
26. V.K. Gupta, B. Gupta, A. Rastogi, S. Agarwal and A. Nayak, *J. Hazard. Mater.*, **186**, 891 (2011).
27. G. Atun, G. Hisarli, W.S. Sheldrick and M. Muhlerler, *J. Colloid Interf. Sci.*, **261**, 32 (2003).
28. T.W. Weber and P. Chakkravorti, *AIChE J.*, 220 (1974).
29. Y.S. Ho and G. McKay, *J. Environ Sci. Health A*, **34**, 1179 (1999).
30. A. Ozer, G. Akkaya and M. Turabik, *Chem. Eng. J.*, **112**, 181 (2005).
31. A. Ozcan and A.S. Ozcan, *J. Hazard. Mater. B*, **125**, 252 (2005).
32. L. Zhoua, J. Jin, Z. Liu, X. Liang and C. Shang, *J. Hazard. Mater*., **185**, 1045 (2011).
33. D. Prahas, Y. Kartika, N. Indraswati and S. Ismadji, *Chem. Eng. J.*, **140**, 32 (2008).
34. N.F. Cardoso, E.C. Lima, I.S. Pinto, C.V. Amavisca, B. Royer, R.B. Pinto, W.S. Alen-car and S.F.P. Pereira, *J. Environ. Manage.*, **92**, 1237 (2011).
35. Y.S. Ho, *J. Hazard. Mater.*, **136**, 681 (2006).
36. F. Ahmad, W.M.A.W. Daud, M.A. Ahmad and R. Radzi, *Chem. Eng. J.*, **178**, 461 (2011).